



CHORUS

This is the accepted manuscript made available via CHORUS. The article has been published as:

Anomalous charge and negative-charge-transfer insulating state in cuprate chain compound KCuO_2

D. Choudhury, P. Rivero, D. Meyers, X. Liu, Y. Cao, S. Middey, M. J. Whitaker, S. Barraza-Lopez, J. W. Freeland, M. Greenblatt, and J. Chakhalian

Phys. Rev. B **92**, 201108 — Published 19 November 2015

DOI: [10.1103/PhysRevB.92.201108](https://doi.org/10.1103/PhysRevB.92.201108)

Anomalous charge and negative-charge-transfer insulating state in cuprate chain-compound KCuO_2

D. Choudhury,^{1,2,*} P. Rivero,¹ D. Meyers,¹ X. Liu,¹ Y. Cao,¹ S. Middey,¹ M. J. Whitaker,³ S. Barraza-Lopez,¹ J. W. Freeland,⁴ M. Greenblatt,³ and J. Chakhalian¹

¹*Department of Physics, University of Arkansas, Fayetteville, AR 72701, USA*

²*Department of Physics, Indian Institute of Technology, Kharagpur 721302, INDIA*

³*Department of Chemistry and Chemical Biology, Rutgers University, Piscataway, NJ 08854-8087, USA*

⁴*Advanced Photon Source, Argonne National Laboratory, Argonne, Illinois 60439, USA*

(Dated: November 3, 2015)

Using a combination of X-ray absorption spectroscopy (XAS) experiments and first-principles calculations, we demonstrate that insulating KCuO_2 contains Cu in an unusually-high formal-3+ valence state, the ligand-to-metal (O to Cu) charge transfer energy is intriguingly negative ($\Delta \sim -1.5$ eV) and has a dominant ($\sim 60\%$) ligand-hole character in the ground state akin to the high Tc cuprate Zhang-Rice state. Unlike most other formal Cu^{3+} compounds, the Cu $2p$ XAS spectra of KCuO_2 exhibits pronounced $3d^8$ (Cu^{3+}) multiplet structures, which accounts for $\sim 40\%$ of its ground state wave-function. *Ab initio* calculations elucidate the origin of the band-gap in KCuO_2 as arising primarily from strong intra-cluster Cu $3d$ - O $2p$ hybridizations (t_{pd}); the value of the band-gap decreases with reduced value of t_{pd} . Further, unlike conventional negative charge-transfer insulators, the band-gap in KCuO_2 persists even for vanishing values of Coulomb repulsion U , underscoring the importance of single-particle band-structure effects connected to the one-dimensional nature of the compound.

PACS numbers: 71.30.+h, 78.70.Dm, 71.27.+a, 71.15.Mb

The electronic properties of strongly correlated transition metal (TM) oxides –which consist of partially filled TM d -orbitals hybridized with the ligand (oxygen) p -orbitals– are effectively categorized under the well known Zaanen-Sawatzky-Allen (ZSA) phase diagram [1–3], a guiding principle for materials scientists that takes into consideration the on-site d - d Coulomb interaction energy at the TM site (U) and the ligand-to-TM charge transfer energy (Δ). There is an intriguing region of the ZSA phase diagram of compounds with negative values of Δ that has been less explored [4–10]. In TM oxides the value of Δ decreases by increasing the valence (oxidation) state of the TM ion, and for unusual high valence states Δ can even become negative [8]. Such high-valence compounds are very unstable, and only a few pristine negative Δ compounds exist (see Table I). For such highly covalent compounds, it is energetically favorable to transfer an electron from the ligand to the metal ion, as the energy cost Δ for this process is negative, giving rise to a large *ligand-hole* character and usually metallic nature of the ground state. However, there exists a very select number of compounds, which are insulating while having negative or extremely small values of Δ , driven by a combination of strong metal-ligand hybridization either with strong electronic correlations, as in the case of the correlated covalent insulators [4, 6, 15, 16], like in Sr_2CuO_3 [17], or describable within an effective single-particle band-structure, as in the case of NaCuO_2 [5, 7, 8, 15, 18, 19].

In this work, using X-ray absorption spectroscopy (XAS) experiments, model XAS and density functional theory (DFT) calculations, we have investigated the electronic structure of KCuO_2 [21], and have elucidated the nature of its experimentally observed insulating state. Our results suggest that KCuO_2 hosts Cu in a formal 3+ valence state, has a negative Δ and a dominant ligand-hole character on its ground state.

Table I. Coulomb repulsion U and charge-transfer Δ energies (in units of eV) for some transition metal oxides with unusually high formal-valence states for the B site (Fe, Co, Ni, Cu) cation.

Compound	Formal-valence	U	Δ	Transport	Ref.
SrFeO_3	(4+)	7.8	0.0	Metal	[2]
BaFeO_3	(4+)	7.1	-0.9	Insulator	[11]
SrCoO_3	(4+)	7.0	-5.0	Metal	[12]
LaNiO_3	(3+)	7.0	1.0	Metal	[13]
LaCuO_3	(3+)	7.0	-1.0	Metal	[14]
NaCuO_2	(3+)	8.0	-2.5	Insulator	[7]
KCuO_2	(3+)	8.0	-1.5	Insulator	this work

We find a charge band gap (~ 1.24 eV) with preponderance of O $2p$ states at the valence band and conduction band edges, which originates from strong intra-cluster Cu $3d$ - O $2p$ hybridization in this negative Δ compound and competes with point-charge Coulomb contributions to the crystal-field energies of the Cu t_{2g} orbitals. The chain-topology driven band-gap persists for vanishing U , which is distinct from the conventional picture of correlated covalent insulators [4, 6, 15], and also decreases with decreasing values of t_{pd} . The inclusion of additional electron-electron correlations with the use of a non-negligible value of U is, however, necessary to account for the experimental value of the gap. Our work thus establishes that KCuO_2 , similar to NaCuO_2 , is a negative Δ insulator where the insulating behavior arises from single-particle band structure effects from the unique one-dimensional CuO_2 chain geometry and electron-electron correlations accounted for within an effective U term.

Methods (experimental).— Single-phase polycrystalline KCuO_2 was synthesized in an orthorhombic $Cmcm$ space

group by mixing KO_2 and CuO powders in a 1:1 ratio in an Ar-filled glovebox followed by sintering under a dry O_2 atmosphere for 2.5 days at 450°C [22]. XA measurements at $\text{Cu } L_{2,3}$ - and $\text{O } K$ -edges were performed on the 4-ID-C beam line of the Advanced Photon Source (APS) at Argonne National Laboratory, USA. The sample powder was mounted on the holder using carbon-tape under a nitrogen gas atmosphere to ensure minimum exposure to air, and XAS measurements in total-electron-yield (TEY), total-fluorescence-yield (TFY), and in the inverse-partial-fluorescence-yield (IPFY) modes were performed at room temperature without any additional surface preparation. The probing depth in case of the TEY (~ 5 nm) is much smaller than that of TFY or IPFY (~ 100 nm)[23], and thus, while TEY studies the under-coordinated surface electronic-structure of a solid, the TFY and IPFY are well-suited to investigate the bulk electronic-structure. The non-resonant $\text{O } K$ -edge was monitored during IPFY measurements: these IPFY measurements are further free from any self-absorption effects that may still be present in the TFY spectra [24].

Methods (theory).— We have performed three sets of complementary calculations. To act as a reference XAS spectra, calculations of the $\text{Cu } L_{2,3}$ XA spectrum on a orthorhombic $Cmcm$ space-group lattice of KCuO_2 [25] (e.g., Figs. 1(a-b)) were performed using the Finite Difference Method Near-Edge Structure (FDMNES) code [26]. The FDMNES calculations were performed using the full-multiple-scattering theory with a cluster radius of 6 \AA around the absorbing Cu atom and an on-site Coulomb energy (U) of 8 eV.

In order to determine the relative TM-O covalencies, cluster calculations for simulating the $\text{Cu } L_{2,3}$ XA spectrum of a single CuO_2 planar-cluster with a D_{4h} symmetry [27] were performed using the Charge Transfer Multiplet program for X-ray Absorption Spectroscopy (CTM4XAS) [28]. The charge transfer energy Δ between $\text{Cu } 3d$ and $\text{O } 2p$ orbitals is defined as $E(d^{n+1}\underline{L}) - E(d^n)$, where $E(d^n)$ is the multiplet-averaged energy for n -electron occupancy on $\text{Cu } 3d$ levels and $E(d^{n+1}\underline{L})$ denotes the multiplet-averaged energy obtained after transferring one electron from an $\text{O } 2p$ level to the $\text{Cu } 3d$ level having $n=8$ electrons, corresponding to the formal (3+) valence state of Cu. For the CTM4XAS calculations, the basis size was restricted up to one electron charge-transfer from $\text{O } 2p$ to $\text{Cu } 3d$.

To determine the density of states (DOS) of KCuO_2 and NaCuO_2 , the rotationally invariant LDA+U scheme of Dudarev *et al.* [29] was employed in DFT electronic structure calculations. Calculations were carried out with the Vienna *Ab initio* Simulation Package (VASP) [30] using projector-augmented wave pseudopotentials [31, 32]. The first Brillouin zone was sampled using a $12 \times 12 \times 6$ Monkhorst-Pack set of k-points and a 400 eV energy cutoff.

Results and discussion.— Two distinct groups of experimentally-observed XAS peaks, one around 930 eV (L_3 region) and another group around 950 eV (L_2 region) can be clearly identified for the $\text{Cu } L_{2,3}$ -edge of KCuO_2 (c.f., Fig. 1(c)). While the spectral features for the L_3 and L_2

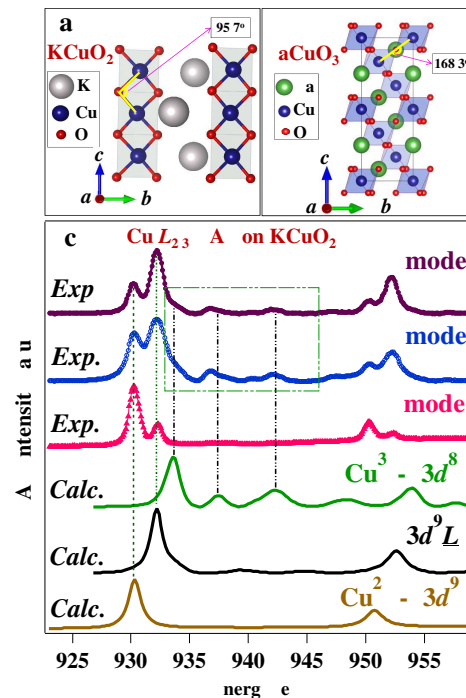


Figure 1. (Color online) Schematic crystal structures showing (a) edge-sharing of CuO_4 units in KCuO_2 and (b) corner-sharing of CuO_6 clusters for LaCuO_3 . (c) $\text{Cu } L_{2,3}$ X-ray absorption (XA) spectra of KCuO_2 collected in the inverse-partial-fluorescence-yield (IPFY), the total-fluorescence-yield (TFY) and the total-electron-yield (TEY) modes. Calculated XA spectra (solid lines) of KCuO_2 with the FDMNES code for $3d^9$, $3d^8$ and $3d^9 \underline{L}$ configurations are also shown.

regions are nearly identical, they are separated by about 20 eV due to the $3/2 \times \text{Cu } 2p$ core-spin-orbit coupling. Looking around the $\text{Cu } L_3$ region closely, we observe two intense peaks at 930.3 eV and 932.3 eV, which correspond to the $\text{Cu } d^9$ and the $\text{Cu } d^9 \underline{L}$ initial states, respectively [33–35].

The d^9 (Cu^{2+}) peak intensity increases significantly in the TEY mode as compared to the TFY and IPFY modes, indicating an abundance of Cu^{2+} valence states on the surface (see Methods section). This Cu^{2+} presence is believed to arise due to the presence of surface impurity phases rich in Cu^{2+} . Note that similar peaks of d^9 (Cu^{2+}) have been observed for other formally Cu^{3+} compounds in the XA spectrum (e.g., NaCuO_2 [5, 8, 33], $\text{CaCu}_3\text{Co}_4\text{O}_{12}$ [35] and Cs_2KCuF_6 [36]). Cu^{2+} impurity phases on the surfaces of these metastable compounds arises due to the loss of superficial anionic atoms during XAS experiments in ultra-high vacuum which effectively reduces the valence of surrounding Cu ions [8]. Further, we observed that KCuO_2 on exposure to air decomposes into CuO within five to ten minutes. Thus, given these constraints, it is impossible for us to avoid the Cu^{2+} related impurity peak in the XAS experiments. Within the bulk, KCuO_2 is not expected to suffer from such anionic losses and, accordingly, much lower intensity Cu^{2+} peaks in the bulk-sensitive TFY and IPFY XAS spectra are observed in Fig. 1(c). Some per-

centage of the TFY and IPFY signals are also contributed from the surface and near-surface region of the sample, which is dominant due to powder nature of KCuO_2 sample as compared to scraped bulk-polycrystalline pellet of NaCuO_2 [33], that still provides significant contributions of the d^9 peak. The differences in relative spectral weights among IPFY and TFY data [37] are assigned to known self-absorption effects [24] on the TFY spectra.

Focussing henceforth on the IPFY spectrum, as it is both bulk-sensitive and free from self-absorption effects, the main peak given by the $d^9 \underline{L}$ state arises due to the charge transfer of an electron from the surrounding O atoms into formally $\text{Cu } 3d^8$ (Cu^{3+}) state [33–35]. Furthermore, distinct multiplet-structures –that are considered to provide clear evidence for the presence of an ionic Cu^{3+} (d^8) state [33–35]– are observed around 940 eV. The presence of significant $d^9 \underline{L}$ and d^8 intensities suggests that a coherent superposition of both states constitutes the ground state of formal Cu^{3+} ions in KCuO_2 , similar to that of NaCuO_2 [33]. It is important to note that on a $\text{Cu } 2p$ - $3d$ XAS process it is difficult to detect contributions from the $d^{10} \underline{L}^2$ level to the ground-state. However, such contributions are usually small, as determined by X-ray photo-electron spectroscopy on related systems [8].

To further establish the origin of the various features in the experimental XAS spectra, we simulated the $\text{Cu } L_{2,3}$ XAS spectra of KCuO_2 that corresponds to the d^8 , d^9 and $d^9 \underline{L}$ initial state configurations using the FDMNES code. As shown by the vertical guide lines in Fig. 1(c), the calculated XAS spectra corresponds to the d^9 and $d^9 \underline{L}$ features in the experimental spectra, and the observed ionic d^8 - experimental features can be broadly understood with the calculated spectrum for the d^8 ionic Cu^{3+} state.

We now compare the L_3 energy region for KCuO_2 with other systems that host unusual valence states of Cu, such as the optimally-doped $\text{YBa}_2\text{Cu}_3\text{O}_{7-\delta}$ (YBCO) [35], LaCuO_3 [35], and NaCuO_2 [33] in Fig. 2(a), after subtraction of the surface Cu^{2+} impurity peak [38, 39]. It is interesting to note that the Zhang-Rice spin-singlet-state, $d^9 \underline{L}$ [40, 41], which arises due to external hole-doping in YBCO by chemical routes [33], naturally becomes the dominant state in formally Cu^{3+} compounds. This hole-doping mechanism is akin to a self-doping effect [20]. Judging from the intensity ratios shown in Fig. 2, the $d^9 \underline{L}$ charge-transfer state appears dominant over the ionic d^8 state for KCuO_2 , NaCuO_2 and LaCuO_3 , thus suggesting that the associated charge transfer energies Δ for all of these compounds are unusually *negative*. We note that negative values of Δ have been already proposed for insulating NaCuO_2 [5, 7, 8] and metallic LaCuO_3 [14].

A closer analysis of the XA shapes on Fig. 2(a) points to spectral differences within several formal Cu^{3+} compounds. Let us focus on the differences in the XA spectral features related to the $d^9 \underline{L}$ state first: The $d^9 \underline{L}$ peak for LaCuO_3 is broad and can be well described using two peaks, one centered at 930.8 eV and another at 932.2 eV. This splitting occurs from the delocalization of the ligand-hole, due to inter-cluster hybridization effects that are aided by the corner-sharing geom-

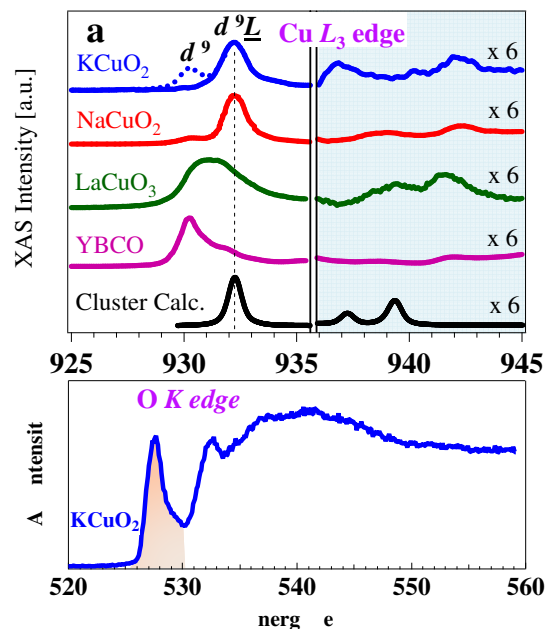


Figure 2. (Color online) (a) $\text{Cu } L_3$ X-ray absorption (XA) spectra of KCuO_2 , NaCuO_2 [33], LaCuO_3 and $\text{YBa}_2\text{Cu}_3\text{O}_{7-\delta}$ (YBCO). The main $\text{Cu } L_3$ peak in KCuO_2 and NaCuO_2 , and the shoulder in YBCO around 932 eV correspond to the $d^9 \underline{L}$ Zhang-Rice singlet state. The d^8 multiplet structures six-fold-increased for easier observation are also shown. The calculated XAS spectrum for a single undistorted CuO_4 cluster of D_{4h} symmetry and corresponding to $\Delta = -1.5$ eV is also shown. (b) The O K -edge XA spectrum of KCuO_2 consists of a pronounced pre-peak around 527.6 eV (shaded area) suggesting a large ligand-hole character of its ground state.

etry of the CuO_6 clusters with Cu-O-Cu bond angle of 168.3° in LaCuO_3 [14] (c.f., Fig. 1(b)). For KCuO_2 and NaCuO_2 , on the other hand, such inter-cluster hybridization effects are negligible due to the near-orthogonal Cu-O-Cu bond-angle (95.7°) between neighboring CuO_4 clusters (c.f., Fig. 1(a)) and a single $d^9 \underline{L}$ peak is observed.

The d^8 multiplet region of formally Cu^{3+} compounds shown by the shaded area in Fig. 2(a) is discussed next. Covalency and Δ are not independent, since the relative intensities between the d^8 multiplets to the $d^9 \underline{L}$ peak usually increase with decreasing covalency, and their energy separation increases with larger negative values of Δ [36]. KCuO_2 has stronger multiplet intensities than iso-structural NaCuO_2 , which suggests a larger contribution of the ionic d^8 state to its ground state. Further, the average energy difference between the d^8 multiplets and the $d^9 \underline{L}$ peak is 5.9 eV and 8.2 eV for KCuO_2 and NaCuO_2 , respectively, thus showing a smaller negative Δ for KCuO_2 .

For the calculated $\text{Cu } L_{2,3}$ XA spectra on a single CuO_4 cluster with planar D_{4h} symmetry [42], we optimized the parameter values to match the calculated energy separations between the average d^8 multiplets and the $d^9 \underline{L}$ main peak with energy differences obtained from experiment (Fig. 2(a)). The estimated Δ , thus obtained, turned out to be -1.5 eV

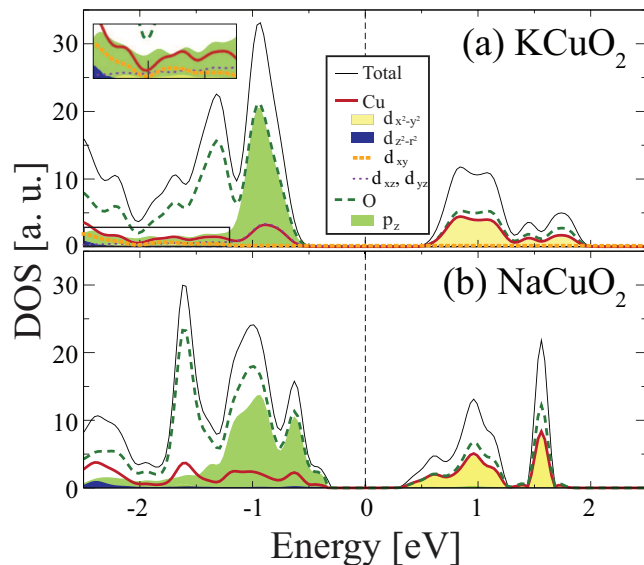


Figure 3. (Color online) Density of states for (a) KCuO_2 and (b) NaCuO_2 ; the total contributions from a given atomic species are indicated by trendlines and the orbital projections are shown by colored area plots. A U of 8 eV was used for these calculations. KCuO_2 is found to exhibit a larger bandgap than NaCuO_2 .

and -2.5 eV for KCuO_2 and NaCuO_2 respectively. Furthermore, both the resultant ground states have dominant $d^9 \underline{L}$ characters, $39\%d^8 + 61\%d^9 \underline{L}$ ($36\%d^8 + 64\%d^9 \underline{L}$) for KCuO_2 (NaCuO_2), with a higher ionic character for the ground state of KCuO_2 , as suggested earlier.

The O K -edge XA spectrum – which probes the ligand hole-states – exhibits a pronounced pre-peak for KCuO_2 at 527.6 eV, as seen in Fig. 2(b). The intensity of the O K -edge pre-peak correlates directly with the amount of ligand-hole character in the ground state [36], thus the strong pre-peak in KCuO_2 further establishes a large $d^9 \underline{L}$ character of its ground state.

Fig. 3 shows the density of states (DOS) projected onto orbital contributions for KCuO_2 and NaCuO_2 , which were found to have insulating gaps of 1.24 eV and 0.62 eV respectively for the U value of 8 eV. The band-gaps in KCuO_2 and NaCuO_2 , however, exist even for $U = 0$ eV, in agreement with previous observations on NaCuO_2 [7, 15, 18], highlighting the role of single-particle band-structure effects due to the chain topology in giving rise to the insulating state in KCuO_2 . The inclusion of correlations, however, is essential in increasing the band-gap value as compared to $U = 0$ eV and bringing it to the agreement with the experimental value [8]. Furthermore, the projected DOS shows a strong O character in both valence and conduction band edges [43]. The Cu t_{2g} levels occur between the lower-lying $3d_{3z^2-r^2}$ and higher-lying $3d_{x^2-y^2}$ levels, as usually observed for one-dimensional CuO_2 chains due to point charge (Coulomb) contribution [44]. However, the t_{2g} levels is intriguingly seen to have Cu (d_{xz}) and Cu(d_{yz}) character immediately below E_F and Cu d_{xy} character only at further lower energies, which is different

from a point charge (Coulomb) contribution to crystal-field splitting. Similar effect has been observed in $\text{Cs}_2\text{Au}_2\text{Cl}_6$, and arises from a dominant pd covalency contribution in case of negative Δ compounds [10]; the inversion of the t_{2g} orbitals thus further confirms the negative Δ in KCuO_2 .

We also performed a Bader analysis [45] to understand the charge density distribution over electronic orbitals. The total occupation of Cu $3d$ -shell in both systems is 8.8, which represents a mixture of d^8 and d^9 states, in qualitative agreement with cluster calculations and establishing the superposition of both contributions to the ground state of formally Cu^{3+} ions in KCuO_2 and NaCuO_2 , as discussed earlier.

Conclusions. – We have described the presence of the anomalous charge state of Cu in KCuO_2 from experiment and theory. We established the negative charge transfer energy of the KCuO_2 ground state and its dominant ligand-hole character, which arise due to large intra-cluster hybridization effects and remain localized due to weak inter-cluster hybridizations. Localized cuprate like Zhang-Rice singlet state thus occur at every unit cell, which consequently gives rise to the experimentally observed insulating and diamagnetic character of KCuO_2 [20, 21]. Moreover, KCuO_2 exhibits strong d^8 related multiplet structures, resulting from the large ionic Cu^{3+} character of its ground-state. KCuO_2 is shown to belong to the unusual class of covalency driven negative charge transfer with the correlated gap that is adiabatically connected to the single-particle gap arising the chain geometry of the compound.

We deeply thank D. D. Sarma and D. I. Khomskii for insightful suggestions and comments. We thank NSF-XSEDE (Grant TG-PHY090002; TACC’s *Stampede*) and HPC at Arkansas for computational support. JC was funded by the Gordon and Betty Moore Foundation’s EPIQS Initiative through Grant GBMF4534. SM and DM were funded by the DOD-ARO under Grant No. 0402-17291 for the synchrotron work at APS. Work at the Advanced Photon Source is supported by the U.S. Department of Energy, Office of Science under grant No. DEAC02-06CH11357. P.R. and S.B.L. acknowledge funding from the Arkansas Biosciences Institute.

* debraj@phy.iitkgp.ernet.in

- [1] J. Zaanen, G. A. Sawatzky, and J. W. Allen *Phys. Rev. Lett.* **55**, 418 (1985).
- [2] A. E. Bocquet, T. Mizokawa, T. Saitoh, H. Namatame, and A. Fujimori *Phys. Rev. B* **46**, 3771 (1992).
- [3] A. E. Bocquet, T. Mizokawa, K. Morikawa, A. Fujimori, S. R. Barman, K. Maiti, D. D. Sarma, Y. Tokura, and M. Onoda *Phys. Rev. B* **53**, 1161 (1996).
- [4] D. D. Sarma *J. Solid State Chem.* **88**, 45 (1990).
- [5] T. Mizokawa, H. Namatame, A. Fujimori, K. Akeyama, H. Kondoh, H. Kuroda, and N. Kosugi *Phys. Rev. Lett.* **67**, 1638 (1991).
- [6] D. D. Sarma, H. R. Krishnamurthy, S. Nimkar, S. Ramasesha, P. P. Mitra, and T. V. Ramakrishnan *Pramana - J. Phys.* **38**, L531 (1992).

- [7] S. Nimkar, D. D. Sarma, and H. R. Krishnamurthy *Phys. Rev. B* **47**, 10927 (1993).
- [8] T. Mizokawa, A. Fujimori, H. Namatame, K. Akeyama, and N. Kosugi *Phys. Rev. B* **49**, 7193 (1994).
- [9] M. Imada, A. Fujimori, and Y. Tokura *Rev. Mod. Phys.* **70**, 1039 (1998).
- [10] A. V. Ushakov, S. V. Streltsov, and D. I. Khomskii *J. Phys.: Condens. Matter* **23**, 445601 (2011).
- [11] T. Tsuyama, T. Matsuda, S. Chakraverty, J. Okamoto, E. Ikegami, A. Tanaka, T. Mizokawa, H. Y. Hwang, Y. Tokura, and H. Wadati *Phys. Rev. B* **91**, 115101 (2015).
- [12] R. H. Potze, G. A. Sawatzky, and M. Abbate *Phys. Rev. B* **51**, 11501 (1995).
- [13] M. Abbate, G. Zampieri, F. Prado, A. Caneiro, J. M. Gonzalez-Calbet, and M. Vallet-Regi *Phys. Rev. B* **65**, 155101 (2002).
- [14] T. Mizokawa, T. Konishi, A. Fujimori, Z. Hiroi, M. Takano, and Y. Takeda *J. Electron. Spectrosc. Relat. Phenom.* **92**, 97 (1998).
- [15] S. Nimkar, N. Shanthi, and D. D. Sarma *Proc. Indian Acad. Sci. (Chem. Sci.)* **106**, 393 (1994).
- [16] D. D. Sarma, and A. Taraphder *Phys. Rev. B* **39**, 11570 (1989).
- [17] K. Maiti, D. D. Sarma, T. Mizokawa, and A. Fujimori *Europhys. Lett.* **37**, 359 (1997).
- [18] D. J. Singh *Phys. Rev. B* **49**, 1580 (1994).
- [19] D. I. Khomskii *Lithuanian J. Phys.* **37**, 65 (1997) (also in arXiv:cond-mat/0101164).
- [20] D. I. Khomskii *Transition Metal Compounds* (Cambridge University Press, 2014).
- [21] G. A. Costa, and E. Kaiser *Thermochimica Acta* **269/270**, 591 (1995).
- [22] Please refer to Supplementary material for powder X-ray diffraction data analysis and unit-cell parameters.
- [23] S. B. Ogale, T. V. Venkatesan, and M. Blamire *Functional Metal Oxides: New Science and Novel Applications* (Wiley-VCH, 2013).
- [24] A. J. Achkar, T. Z. Regier, E. J. Monkman, K. M. Shen, and D. G. Hawthorn *Sci. Rep.* **1**, 182 (2011).
- [25] K. Hestermann and R. Hoppe *Z. Anorg. Allg. Chem.* **367**, 249 (1969).
- [26] O. Bunau, and Y. Joly *J. Phys. : Condens. Matter* **21**, 345501 (2009).
- [27] Such single-cluster model XA calculations apply reasonably well in case of insulating compounds, especially KCuO_2 and NaCuO_2 , where inter-cluster hybridization effects can be neglected.
- [28] E. Stavitski, and F. M. F. de Groot *Micron* **41**, 687 (2010).
- [29] S. L. Dudarev, G. L. Botton, S. Y. Savrasov, C. J. Humphreys, and A. P. Sutton. *Phys. Rev. B* **57**, 1505 (1998).
- [30] G. Kresse, and J. Furthmüller. *Phys. Rev. B* **54**, 11169 (1996).
- [31] P. E. Blochl *Phys. Rev. B* **50**, 17953 (1994).
- [32] G. Kresse, D. Joubert. *Phys. Rev. B* **59**, 1758 (1999).
- [33] D. D. Sarma, O. Strelbel, C. T. Simmons, U. Neukirch, G. Kaindl, R. Hoppe, and H. P. Müller *Phys. Rev. B* **37**, 9784 (1988).
- [34] R. Sarangi, N. Aboeella, K. Fujisawa, W. B. Tolman, B. Hedman, K. O. Hodgson, and E. I. Solomon *J. Am. Chem. Soc.* **128**, 8286 (2006).
- [35] D. Meyers, S. Mukherjee, J. G. Cheng, S. Middey, J. S. Zhou, J. B. Goodenough, B. A. Gray, J. W. Freeland, T. S. Dasgupta, and J. Chakhalian *Scientific Reports* **3**, 1834 (2013).
- [36] Z. Hu, G. Kaindl, S. A. Warda, D. Reinen, F. M. F. de Groot, and B. G. Müller *Chem. Phys.* **232**, 63 (1998).
- [37] The d^9 peak in the TFY spectra does not suffer from self-absorption effects as the impurity phases containing Cu^{2+} ions lie only over the sample surfaces. However, self-absorption effects affect the $d^9 L$ TFY peak intensity, since it arises from formal Cu^{3+} ions present in high concentrations and spread over the bulk of the sample.
- [38] An arc-tangent background function was subtracted from the spectra first, followed by multi-peak-fitting analysis of the L_3 edge; the peak corresponding to Cu^{2+} (shown with the dashed line in Fig. 2(a)) was subtracted subsequently.
- [39] The XA spectrum of NaCuO_2 in Fig. 2(a) is taken from Ref. [33].
- [40] H. Eskes, and G. A. Sawatzky *Phys. Rev. Lett.* **61**, 1415 (1988).
- [41] F. C. Zhang, and T. M. Rice *Phys. Rev. B* **37**, 3759 (1988).
- [42] D_{4h} effective ligand field parameters: $10D_q = 2.5$ eV, $D_t = 0.24$ eV, $D_s = 0.19$ eV; and Coulomb correlations $U_{dd}=8.0$ eV and $U_{pd} = 10.5$ eV were used. The metal-ligand mixing interaction (T_{B1g}) optimized to -2.42 eV and -3.46 eV was used for KCuO_2 and NaCuO_2 , respectively.
- [43] Due to the extended nature of the O p orbitals, the decomposition of the total DOS by projecting on the LAPW spheres is known to underestimate the O p character [18], thus the valence and conduction bands have larger O p character than that obtained under the LDA+U scheme.
- [44] M. M. Sala, V. Bisogni, C. Aruta, G. Balestrino, H. Berger, N. B. Brookes, G. M. de Luca, D. D. Castro, M. Groni, M. Guarise, P. G. Medaglia, F. M. Granozio, M. Minola, P. Perna, M. Radovic, M. Salluzzo, T. Schmitt, K. J. Zhou, L. Braicovich, and G. Ghiringhelli *New J. of Phys.* **13**, 043026 (2011).
- [45] R. F. W. Bader *Atoms in Molecules: A Quantum Theory* (Oxford University Press, 1990).